Matrix Isoperimetry and Diffusion from Forgotten Order in Block–Zeno Dynamics

Sharp qudit action laws, an exact permutation covariance, and a bounded-clock no-go

Lluis Eriksson

10 August 2026

Abstract

A balanced ordered loop of retained Hamiltonians generates the geometric term

$$H_\sigma = -\frac{i}{2}\sum_{s>r}[h_{\sigma_s}, h_{\sigma_r}].$$

For qubits this is an oriented polygon area. We solve the higher-rank problem and then determine what becomes of the curvature when the order record is erased. For every block size and every $m \geq 3$, define the gauge-invariant operator action

$$S_* = \sum_j \operatorname{dist}(h_j, \mathbb{R}\mathbf{1}) = \frac{1}{2}\sum_j \operatorname{osc}(h_j).$$

If $\sum_j h_j$ is scalar, then the dimension-free sharp inequality

$$\operatorname{osc}(H_\sigma) \leq \frac{S_*^2}{m\tan(\pi/m)}$$

holds. Its constant is attained in every dimension $d \geq 2$ by a regular two-level polygon; order versus reverse attains the sharp relative factor two. A target-sensitive companion bound for Hilbert–Schmidt action is

$$\left(\sum_j \operatorname{dist}_2(h_j, \mathbb{R}\mathbf{1})\right)^2 \geq 2m\tan(\pi/m)\,\|H_\sigma\|_1\,,$$

with equality exactly for blockwise sign-paired nonzero spectra. These results give exact diamond-norm ceilings for order discrimination and close the qudit action problem left open by the qubit theory.

Now draw σ uniformly and retain only its holonomy. With $C_{jk} = i[h_j, h_k]$ and inversion signs $\varepsilon_\sigma(j,k)$, one has the exact curvature-frame identity

$$\mathbb{E}H_\sigma = 0, \qquad \mathbb{E}\,|H_\sigma\rangle\langle H_\sigma| = \frac{1}{12}\sum_{j<k}|C_{jk}\rangle\langle C_{jk}|.$$

Consequently the reversal-symmetric random-unitary product converges in diamond norm at rate $O(n^{-1})$ to the GKLS semigroup generated by

$$\mathcal{Q} = -\frac{1}{24}\sum_{j<k}\operatorname{ad}^2_{C_{jk}}, \qquad \operatorname{Fix}(\mathcal{Q}) = \{C_{jk}\}'.$$

Thus an accessible order label carries conditioned coherent holonomy, whereas forgetting it produces irreversible diffusion governed by the same commutator frame. Finally, in fixed laboratory time T, n cycles of m amplitude-bounded kicks satisfy the sharp clock ceiling

$$\Theta_n \leq \frac{T^2\Lambda^2}{n\,m\tan(\pi/m)};$$

nonzero limiting holonomy requires $\Lambda = \Omega(\sqrt{n})$. Exact qutrit, rank-four, and tetrahedral Pauli certificates accompany the paper.

1 Problem, answer, and novelty boundary

Quantum Zeno dynamics is usually formulated as confinement by rapid measurements [2, 3]. Degenerate nonselective measurements retain a noncommutative block algebra, so a balanced sequence of short kicks can leave a second-order geometric Hamiltonian even when the first-order drift cancels. Holonomies from transported Zeno subspaces are well established [4]; stroboscopic nonselective measurements can also produce semigroup dynamics [5]. The present question is different: what are the exact action and information consequences of the *order* of a fixed-algebra balanced loop?

Two gaps motivate the paper. First, the qubit action law follows from the area of a polygon in $\mathbb{R}^3$, but no vector-area representation survives in general rank. Existing quantum isoperimetric inequalities concern Berry phase and Fubini–Study length [7], while isoholonomic bounds optimize cyclic transport of computational subspaces [8, 9, 10]. Here the projectors are fixed, the path lies in a linear space of retained Hamiltonians, the curvature is an ordered commutator sum, and the operational readout is a diamond norm.

Second, an order label is a record. If it remains on the accessible side of a cut, one has a conditioned Hamiltonian H_σ. If it is discarded, the resulting random-unitary average should be irreversible, but its covariance and fixed algebra are not apparent from generic central-limit reasoning. We derive them exactly from inversion statistics and balance.

The contribution is the conjunction:

(i) a gauge-invariant, dimension-free, sharp operator-action law in arbitrary matrix blocks;

(ii) a target-sensitive trace-norm lower bound for Hilbert–Schmidt action and a classification of its equality spectra;

(iii) exact diamond ceilings and physical state witnesses, with no ancilla needed at the optimum;

(iv) a sharp time–amplitude–cycle frontier exposing a $\sqrt{n}$ control barrier;

(v) an exact 1/12 permutation covariance and an $O(n^{-1})$ twirled GKLS limit;

(vi) a commutator-frame fixed-algebra theorem and a primitive tetrahedral certificate.

Relation to the preceding qubit paper

This manuscript is a sequel to *Operational Curvature of the Heisenberg Cut* [1], not a replacement for it. The preceding paper asks when the order of short pinched words is operationally visible. It establishes the local inversion expansion, the exact diamond readout, contextual invisibility and postselection effects, realizability by three-kick loops, and the sharp action law in a qubit block. The local expansion (18) and the norm identity (16) are recalled here, with a short self-contained derivation, only to connect the new matrix inequalities to channel discrimination.

The results first proved here are the arbitrary-rank operator law in Theorem 4.1, the Hilbert–Schmidt trace-norm law and its equality spectra, the bounded-clock frontier, the exact permutation covariance, the forgotten-order GKLS limit, its commutator-frame fixed algebra, and the reversal-bias and closure estimates. Conversely, the earlier paper's analysis of contextual invisibility, postselection amplification, three-kick universality, and order-conditioned physical Markov semigroups is not repeated. The central questions are therefore different: the earlier work detects a known ordering of physical words, whereas this paper determines the higher-rank synthesis cost and the diffusion that remains after the ordering label is erased.

We do not claim that polygonal isoperimetry [6], inner-derivation norms [11], commutator product formulas [13], higher-order Zeno sequences [14], or random-unitary limits are individually new. The proposed novelty is their exact synthesis around a fixed record algebra and the known-order/forgotten-order dichotomy.

2 Balanced matrix loops and curvature frames

Let

$$\mathcal{H} = \bigoplus_{a=1}^{r} \mathcal{H}_a, \qquad \mathcal{A} = \bigoplus_{a=1}^{r} \mathcal{B}(\mathcal{H}_a), \qquad \mathcal{E}(X) = \sum_a P_a X P_a.$$

For full Hamiltonians H_j, their retained parts are $h_j = \mathcal{E}(H_j) \in \mathcal{A}$. The family is balanced when

$$\sum_{j=1}^{m} h_j \in Z(\mathcal{A}) = \bigoplus_a \mathbb{R}P_a. \tag{1}$$

For a physical order $\sigma = (\sigma_1, \dots, \sigma_m)$, with σ_1 first, define

$$H_\sigma = -\frac{i}{2} \sum_{s>r} [h_{\sigma_s}, h_{\sigma_r}]. \tag{2}$$

Every block of H_σ is traceless. Write

$$C_{jk} = i[h_j, h_k] = C_{jk}^*, \qquad j < k,$$

and let $\varepsilon_\sigma(j,k) = +1$ if j precedes k in σ and -1 otherwise. Then

$$H_\sigma = \frac{1}{2} \sum_{j<k} \varepsilon_\sigma(j,k) C_{jk}. \tag{3}$$

Balance implies the vertex relations

$$\sum_{k \neq j} C_{jk} = 0, \qquad C_{kj} := -C_{jk}. \tag{4}$$

For a Hermitian matrix x, let

$$\operatorname{osc}(x) = \lambda_{\max}(x) - \lambda_{\min}(x), \qquad \operatorname{dist}(x, \mathbb{R}\mathbf{1}) = \frac{1}{2} \operatorname{osc}(x).$$

The equality is the elementary best scalar approximation in operator norm. Define the quotient actions

$$S_*(h) = \sum_j \operatorname{dist}(h_j, Z(\mathcal{A})), \qquad S_2(h) = \sum_j \left\| h_j - \mathcal{E}_Z(h_j) \right\|_2, \tag{5}$$

where the first distance and the center-valued trace $\mathcal{E}_Z$ are taken blockwise. Scalar block energies are gauge and should not be charged.

3 The symplectic polygon lemma

The higher-rank argument rests on a polygon inequality in a complex Hilbert space, not on a three-dimensional cross product.

Lemma 3.1 (complex polygonal area)**.** *Let $x_1, \dots, x_m \in \mathbb{C}^d$, $m \geq 3$, satisfy $\sum_j x_j = 0$, and put $L = \sum_j \|x_j\|$. Then*

$$\left| \sum_{k>j} \operatorname{Im}\langle x_k, x_j \rangle \right| \leq \frac{L^2}{2m \tan(\pi/m)}. \tag{6}$$

The constant is sharp. Equality is attained when the edges form a regular polygon in one complex line.

Proof. Choose an orthonormal basis and write $x_j = (x_j^{(q)})_q$. For every coordinate q, the scalars $x_j^{(q)}$ are the edges of a closed planar m-gon with perimeter

$$L_q = \sum_j |x_j^{(q)}|.$$

The left side of (6) is twice the absolute signed area after summing coordinates. The sharp planar polygonal isoperimetric inequality gives a coordinate contribution at most $L_q^2/[2m\tan(\pi/m)]$. Hence

$$|\mathfrak{a}(x)| \leq \frac{1}{2m\tan(\pi/m)} \sum_q L_q^2.$$

Minkowski's inequality yields

$$\left(\sum_q L_q^2\right)^{1/2} = \left\| \sum_j (|x_j^{(q)}|)_q \right\|_2 \leq \sum_j \|x_j\| = L.$$

The regular one-line polygon gives equality. □

This proof is deliberately coordinate-complete. Projecting a general complex polygon onto one real plane need not preserve its total symplectic area.

4 Dimension-free operator isoperimetry

Theorem 4.1 (sharp qudit action law)**.** *For every balanced m-kick loop in one matrix block,*

$$\boxed{\operatorname{osc}(H_\sigma) \leq \frac{S_*^2}{m\tan(\pi/m)}} \tag{7}$$

for every order σ. The constant is optimal in every dimension $d \geq 2$. In a direct sum of blocks,

$$\operatorname{osc}_{\mathcal{A}}(H_\sigma) := \max_a \operatorname{osc}(P_a H_\sigma P_a) \leq \max_a \frac{S_{*,a}^2}{m\tan(\pi/m)}. \tag{8}$$

Proof. Work in one block and let ψ be a unit eigenvector of H_σ. Choose arbitrary real scalars z_j and set

$$x_j = (\mathbf{1} - |\psi\rangle\langle\psi|)(h_{\sigma_j} - z_{\sigma_j}\mathbf{1})\psi.$$

Balance gives $\sum_j x_j = 0$. Since every h_j is Hermitian, its expectation in ψ is real, and direct expansion of (2) gives

$$\langle\psi, H_\sigma\psi\rangle = \sum_{k>j} \operatorname{Im}\langle x_k, x_j\rangle. \tag{9}$$

Choose each z_j to minimize the operator norm. Then $\sum_j \|x_j\| \leq S_*$. Lemma 3.1 places every eigenvalue of H_σ in

$$\left[-\frac{S_*^2}{2m\tan(\pi/m)}, \frac{S_*^2}{2m\tan(\pi/m)}\right],$$

which proves (7).

For sharpness, embed Pauli X, Y in any two-dimensional sector and take

$$h_j = \ell\left(\cos\frac{2\pi j}{m}\,X + \sin\frac{2\pi j}{m}\,Y\right). \tag{10}$$

The loop is balanced, $S_* = m\ell$, and its geometric spectral diameter is $m\ell^2/\tan(\pi/m)$, giving equality. Inert orthogonal sectors do not change either side. □

Corollary 4.2 (relative order and reversal)**.** *For two orders σ, π of the same balanced loop,*

$$\operatorname{osc}(H_\sigma - H_\pi) \le \frac{2S_*^2}{m\tan(\pi/m)}. \tag{11}$$

The constant is sharp: the regular loop (10) and its reverse satisfy $H_{\operatorname{rev}\sigma} = -H_\sigma$ and attain equality.

The continuum switch limit is finite:

$$\lim_{m\to\infty} m\tan(\pi/m) = \pi. \tag{12}$$

No number of switches can reduce the absolute action price below $S_* \ge \sqrt{\pi \operatorname{osc}(H_\sigma)}$.

5 A target-sensitive Hilbert–Schmidt law

The operator law is complete for a prescribed spectral diameter. Hilbert–Schmidt action sees the full target spectrum and admits a complementary nuclear-norm obstruction.

Theorem 5.1 (trace-norm matrix isoperimetry)**.** *Let $F = H_\sigma$ for a balanced loop and let S_2 be defined by (5). Then*

$$\boxed{S_2^2 \ge 2m\tan(\pi/m)\,\|F\|_1\,.} \tag{13}$$

Equality is attainable if and only if, within every active block, the nonzero spectrum of F is sign-paired:

$$(s_1, \dots, s_q, -s_1, \dots, -s_q), \qquad s_j > 0, \tag{14}$$

with arbitrary additional zeros.

Proof. After subtracting center-valued traces, assume $\sum_j h_j = 0$. Let $Q = P_+(F)$ be the positive spectral projection and define the antisymmetric form on Hermitian matrices

$$\omega_Q(X,Y) = \operatorname{Tr}(Q(-i[X,Y])).$$

Its Hilbert–Schmidt comass is one. Indeed, in the $Q \oplus (1-Q)$ decomposition, $-i[Q,X]$ retains only the off-diagonal block and

$$|\omega_Q(X,Y)| = |\operatorname{Tr}((-i[Q,X])Y)| \le \|X\|_2\,\|Y\|_2\,.$$

The same coordinate-plane proof as Lemma 3.1 gives

$$|\operatorname{Tr}(QF)| \le \frac{S_2^2}{4m\tan(\pi/m)}. \tag{15}$$

Because F is traceless, $\operatorname{Tr}(QF) = \operatorname{Tr}(F_+) = \|F\|_1/2$, proving (13).

Equality in (15) requires a regular polygon in a comass-saturating plane. Such a plane is spanned by

$$X = \begin{pmatrix} 0 & B \\ B^* & 0 \end{pmatrix}, \qquad Y = -i[Q,X].$$

The commutator $i[X,-Y]$ has nonzero eigenvalues equal to the eigenvalues of BB^* and their negatives. Hence equality forces (14). Conversely, for any paired spectrum choose the singular values of B to be $\sqrt{s_j}$ and use a regular coefficient polygon in $\operatorname{span}\{X,-Y\}$. Its scale can be chosen to enclose unit area, and direct calculation gives equality in (13). □

For matrix units E_{ab}, set

$$X_{ab} = \frac{E_{ab} + E_{ba}}{\sqrt{2}}, \qquad Y_{ab} = \frac{-i(E_{ab} - E_{ba})}{\sqrt{2}}.$$

For a qutrit, the square $X_{12}, -Y_{12}, -X_{12}, Y_{12}$ gives

$$F = \operatorname{diag}(1, -1, 0), \qquad S_2^2 = 16.$$

The right side of (13) is also $2 \cdot 4 \cdot \|F\|_1 = 16$. In rank four, a square with two orthogonal root planes gives $F = \operatorname{diag}(2, 1, -2, -1)$ and $S_2^2 = 48$. A spectrum such as $(2, -1, -1)$ is not sign-paired, so the universal lower bound is strict; we make no formula claim for its exact minimum.

6 Diamond curvature and a physical witness

For a fixed block pinching $\mathcal{E}$ and block-diagonal Hermitian F, the classical inner-derivation norm identity [11] becomes

$$\|-i \operatorname{ad}_F \mathcal{E}\|_\diamond = \operatorname{osc}_{\mathcal{A}}(F). \tag{16}$$

The upper bound follows by subtracting block-central spectral midpoints and applying the completely bounded amplification of the inner-derivation identity. For the lower bound, choose extreme eigenvectors u_+, u_- in a maximizing block and the physical state

$$|\psi\rangle = \frac{|u_+\rangle + |u_-\rangle}{\sqrt{2}}. \tag{17}$$

Then

$$\|-i[F, |\psi\rangle\langle\psi|]\|_1 = \lambda_{\max}(F) - \lambda_{\min}(F).$$

Thus no ancilla is required to attain (16). The accompanying SDP uses the general completely bounded norm formulation of Watrous [12] as an independent audit, not as the proof.

For the fixed-record words $W_\sigma(\tau)$ of short kicks, the local permutation expansion is

$$W_\sigma(\tau) - W_\pi(\tau) = -i\tau^2 \operatorname{ad}_{H_\sigma - H_\pi} \mathcal{E} + O_\diamond(\tau^3). \tag{18}$$

Combining (11), (16), and equal-prior channel discrimination gives the sharp resource ceiling

$$p_{\text{succ}}(\tau) - \frac{1}{2} \le \frac{\tau^2 S_*^2}{2m \tan(\pi/m)} + O(\tau^3). \tag{19}$$

Regular two-level order/reversal loops attain the leading constant.

7 The bounded-clock no-go

The diffusive scaling $\tau \sim n^{-1/2}$ keeps a second-order holonomy finite, but it also makes the laboratory duration of n cycles grow as $\sqrt{n}$ when every kick lasts τ. A fixed physical clock reveals a different constraint.

Theorem 7.1 (sharp clock ceiling)**.** *Repeat a balanced m-kick loop for n cycles. Let every kick last δ, let*

$$\operatorname{dist}(h_j, \mathbb{R}\mathbf{1}) \le \Lambda, \qquad T = nm\delta,$$

and define the accumulated second-order curvature

$$\Theta_n = \operatorname{osc}(nH_{\text{geo}}(\delta h_1, \ldots, \delta h_m)).$$

Then

$$\boxed{\Theta_n \le \frac{T^2\Lambda^2}{n\,m\tan(\pi/m)}.} \tag{20}$$

The constant is attained by the regular two-level loop with every kick at amplitude Λ*. Therefore fixed* T *and nonzero target* Θ *require*

$$\Lambda_n \ge \frac{\sqrt{n\,m\tan(\pi/m)\,\Theta}}{T}. \tag{21}$$

Proof. The action of the dimensionless kick edges δh_j is at most $m\delta\Lambda = T\Lambda/n$. Apply Theorem 4.1 and multiply the resulting curvature by n. Equality follows from (10). □

For a purely retained balanced unitary loop, Taylor expansion and telescoping show that the physical n-cycle channel differs from its second-order holonomy approximation by at most $O(n\delta^3m^3\Lambda^3) = O(T^3\Lambda^3/n^2)$. Thus the $1/n$ collapse in (20) is not a remainder artifact. The theorem separates three resources that the formal diffusive parameter alone conflates: elapsed time, Hamiltonian amplitude, and cycle count.

8 Exact covariance of a forgotten order

Let σ be uniform on the permutation group S_m. The inversion signs have zero mean. For three distinct labels $a < b < c$,

$$\mathbb{E}(\varepsilon_{ab}\varepsilon_{ac}) = \mathbb{E}(\varepsilon_{ac}\varepsilon_{bc}) = \frac{1}{3}, \qquad \mathbb{E}(\varepsilon_{ab}\varepsilon_{bc}) = -\frac{1}{3}, \tag{22}$$

while signs on disjoint pairs are uncorrelated.

Theorem 8.1 (curvature-frame covariance)**.** *For every balanced family,*

$$\boxed{\mathbb{E}_\sigma H_\sigma = 0, \qquad \mathbb{E}_\sigma|H_\sigma\rangle\langle H_\sigma| = \frac{1}{12}\sum_{j<k}|C_{jk}\rangle\langle C_{jk}|.} \tag{23}$$

The ket notation denotes Hilbert–Schmidt vectorization, so the second identity is an equality of positive operators on matrix space.

Proof. The mean follows from (3). For the covariance, diagonal pair terms initially contribute $\frac{1}{4}\sum|C_{jk}\rangle\langle C_{jk}|$. Only pairs of edges sharing one label contribute cross terms. Extend C_{jk} antisymmetrically. Equations (22) say that every shared-vertex cross term equals one third of the correspondingly oriented dyad.

Now square the vertex relations (4) in Hilbert–Schmidt space and sum over vertices. Every diagonal edge dyad occurs twice, while every shared-vertex symmetric cross dyad occurs once. Hence the full oriented cross sum is minus twice the diagonal sum. Multiplying by the factor $1/3$ from (22) and the outer factor $1/4$ gives

$$\frac{1}{4}\left(1-\frac{2}{3}\right)\sum_{j<k}|C_{jk}\rangle\langle C_{jk}| = \frac{1}{12}\sum_{j<k}|C_{jk}\rangle\langle C_{jk}|.$$

□

This identity is stronger than a scalar variance. It identifies every anisotropic curvature mode and gives its exact weight.

9 Forgotten order generates quantum diffusion

Suppose the order label is used to generate the effective holonomy H_σ and is then discarded. At scale $s \geq 0$, the accessible channel is

$$\Phi_s = \frac{1}{m!} \sum_{\sigma \in S_m} \mathrm{Ad}_{e^{-i\sqrt{s}H_\sigma}} . \tag{24}$$

Reversal maps H_σ to $-H_\sigma$, so the distribution is centrally symmetric.

Theorem 9.1 (twirled curvature limit)**.** *Define*

$$\boxed{\mathcal{Q} = -\frac{1}{24} \sum_{j<k} \mathrm{ad}^2_{C_{jk}} .} \tag{25}$$

Then for every $t \geq 0$,

$$\Phi^n_{t/n} \longrightarrow e^{t\mathcal{Q}} \quad \textit{in diamond norm at rate } O(n^{-1}). \tag{26}$$

More explicitly, if $R = \max_\sigma \|H_\sigma\|$ and $g = 2R^2$, then

$$\left\| \Phi^n_{t/n} - e^{t\mathcal{Q}} \right\|_\diamond \leq \frac{1}{n} \left(\frac{2}{3} R^4 t^2 + \frac{1}{2} g^2 t^2 e^{gt/n} \right) . \tag{27}$$

Proof. Expand the unitary channel in powers of $\sqrt{s}$:

$$\mathrm{Ad}_{e^{-i\sqrt{s}H}} = e^{-i\sqrt{s}\,\mathrm{ad}_H} .$$

All odd terms vanish after the uniform average because H and $-H$ have equal weight. Theorem 8.1 gives

$$-\frac{1}{2} \mathbb{E}\, \mathrm{ad}^2_{H_\sigma} = -\frac{1}{24} \sum_{j<k} \mathrm{ad}^2_{C_{jk}} = \mathcal{Q}.$$

The fourth-derivative integral remainder is bounded by $\frac{2}{3} R^4 s^2$, since $\|\mathrm{ad}_H\|_\diamond \leq 2\|H\|$. Also $\|\mathcal{Q}\|_\diamond \leq g$, so

$$\left\| e^{s\mathcal{Q}} - (I + s\mathcal{Q}) \right\|_\diamond \leq \frac{1}{2} g^2 s^2 e^{gs} .$$

Telescoping n powers of channels with $s = t/n$ proves (27). The central symmetry is what improves the generic $n^{-1/2}$ rate to n^{-1}. ☐

Each term $-\frac{1}{2}\mathrm{ad}^2_C$ is a dephasing GKLS generator, so (25) is manifestly completely positive and trace preserving at semigroup level. Coherent conditional branches have become an irreversible frame Laplacian solely because the classical order record crossed the accessible cut.

10 Fixed algebra, gap, and imperfect randomization

Theorem 10.1 (commutator-frame fixed algebra)**.** *The fixed algebra of the twirled semigroup is*

$$\mathrm{Fix}(\mathcal{Q}) = \{X : [X, C_{jk}] = 0 \textit{ for every } j < k\} = \{C_{jk}\}' . \tag{28}$$

Moreover

$$-\langle X, \mathcal{Q}X \rangle_{\mathrm{HS}} = \frac{1}{24} \sum_{j<k} \|[C_{jk}, X]\|_2^2 . \tag{29}$$

The smallest positive eigenvalue of the frame operator on the orthogonal complement of (28) is the exact L^2 mixing gap.

Proof. Equation (29) follows by cyclicity of trace. Its right side vanishes exactly on the joint commutant, proving both claims. □

Uniformity can be weakened to any reversal-symmetric distribution $p(\sigma) = p(\operatorname{rev}\sigma)$. Odd moments still vanish, the covariance becomes the corresponding weighted frame, and the $O(n^{-1})$ proof is unchanged. If

$$\epsilon_{\text{rev}} = \|p - p \circ \operatorname{rev}\|_1 ,$$

then the mean holonomy satisfies

$$\|\mathbb{E}_p H_\sigma\| \le \frac{1}{2} R \epsilon_{\text{rev}}. \tag{30}$$

At scale $s = t/n$ this produces an accumulated coherent drift of order $\epsilon_{\text{rev}}\sqrt{n}$. A purely diffusive limit therefore requires $\epsilon_{\text{rev}} = O(n^{-1/2})$, or explicit recentering. This gives a calibration criterion for the order randomizer.

Balance itself has an exact robust closure. For an arbitrary open list, let $B = \sum_{j=1}^{m} h_j$ and append $h_{m+1} = -B$. Then

$$H_{\text{geo}}(h_1, \dots, h_m, -B) = H_{\text{geo}}(h_1, \dots, h_m), \tag{31}$$

because the new cross sum is $[-B, B] = 0$. Thus any balance defect is repaired without altering curvature, at the explicit extra quotient-action cost $\operatorname{dist}(B, \mathbb{R}\mathbf{1})$, after which Theorem 4.1 applies with $m + 1$ edges.

11 Exact tetrahedral architecture

Let X, Y, Z be Pauli matrices and choose four retained kicks

$$\begin{aligned} h_1 &= X + Y + Z, & h_2 &= X - Y - Z, \\ h_3 &= -X + Y - Z, & h_4 &= -X - Y + Z. \end{aligned} \tag{32}$$

They are the vertices of a regular tetrahedron in coefficient space and sum to zero. Exhausting all 24 orderings gives exactly

$$\mathbb{E} H_\sigma = 0, \qquad \mathbb{E}\,\|H_\sigma\|_2^2 = 32. \tag{33}$$

The commutator frame is isotropic and

$$\mathcal{Q}(I) = 0, \qquad \mathcal{Q}(X) = -\frac{64}{3}X, \quad \mathcal{Q}(Y) = -\frac{64}{3}Y, \quad \mathcal{Q}(Z) = -\frac{64}{3}Z. \tag{34}$$

Thus forgotten order produces exact primitive depolarization with fixed algebra $\mathbb{C}I$ and gap $64/3$.

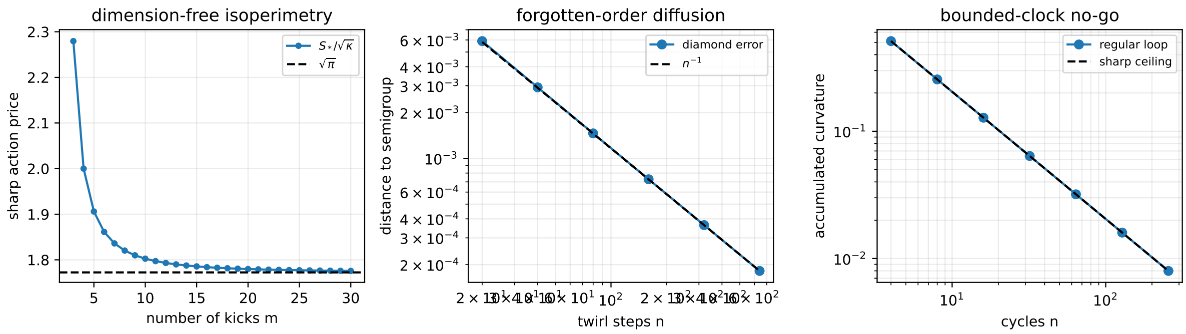

Figure 1: Left: the sharp operator-action price is independent of matrix dimension and tends to $\sqrt{\pi}$. Center: the tetrahedral permutation twirl converges to its GKLS limit at the reversal-improved diamond rate n^{-1}. Right: at fixed laboratory time and amplitude, the regular loop saturates the curvature ceiling and collapses as n^{-1}.

The deterministic replay also checks the covariance identity on generic balanced qutrit families with four and five kicks, tests both matrix inequalities on 600 seeded random qudit loops in dimensions two through seven, and verifies sharp regular embeddings in dimensions two through eight. SymPy independently certifies (33)–(34) and the qutrit/rank-four equality architectures.

Table 1: Representative exact or independently replayed certificates.

Claim	Value	Route
Qutrit target	$\mathrm{diag}(1,-1,0)$	exact SymPy
Qutrit S_2^2 / lower bound	16/16	exact SymPy
Rank-four target	$\mathrm{diag}(2,1,-2,-1)$	exact SymPy
Rank-four S_2^2 / lower bound	48/48	exact SymPy
Uniform covariance coefficient	1/12	24-order exact sum
Tetrahedral $\mathbb{E}\,\lVert H_\sigma\rVert_2^2$	32	exact SymPy
Tetrahedral fixed algebra	$\mathbb{C}I$	commutator frame
Tetrahedral gap	64/3	exact spectrum
Diamond convergence slope	−1.00364	SDP replay
Clock exponent	−1	exact regular loop

12 Interpretation and limits

The results expose two resource transformations. With a known order, H_σ is coherent and its largest operational effect is sharply limited by a matrix perimeter. With the order forgotten, its mean vanishes but its covariance remains; the same commutator family becomes a dissipative frame. In symbols,

$$\begin{aligned}\text{order retained} &\implies H_\sigma \text{ and diamond curvature,}\\ \text{order erased} &\implies -\frac{1}{24}\sum_{j<k}\mathrm{ad}^2_{C_{jk}} \text{ and diffusion.}\end{aligned}$$

This is an operational statement about a classical record, not objective collapse. The accessible channel is random-unitary because the label is traced out.

Several boundaries are explicit. Rank-one record algebras are commutative and have $C_{jk}=0$. The operator action charges retained Hamiltonians modulo the center, not measurement work or off-block couplings. The clock theorem assumes instantaneous measurements and equal kick durations; nonzero measurement duration only tightens a fixed-time budget. The twirl theorem acts on the effective holonomies H_σ and assumes a fresh order draw at every step. Infinite-dimensional and unbounded-generator extensions are not claimed.

The closest geometric results optimize Berry/Fubini–Study paths or transported subspaces [7, 8, 9]; they do not give (7), the inversion covariance (23), or the frame generator (25). Conversely, the present results do not address global band geometry or adiabatic gate holonomy. Higher-order Zeno and commutator formulas [14, 13] can improve implementation errors, but do not remove the sharp action or bounded-clock ceilings.

13 Conclusion

Balanced matrix loops obey a sharp isoperimetric law independent of rank. The operator version gives a complete scalar action–curvature region with universal two-level extremizers; the Hilbert–Schmidt version detects the complete target spectrum and identifies sign-paired equality cases. The same curvature family has an exact permutation covariance. Keeping the order record selects a coherent holonomy, while forgetting it produces a GKLS frame Laplacian whose fixed algebra and gap are explicit. Finally, a fixed physical clock turns the action law into a no-go: constant holonomy under increasingly rapid cycling requires control amplitude growing as $\sqrt{n}$. These results close the higher-rank gap of the qubit theory and turn the location of an order record into a quantitative dynamical resource.

Data and code availability

The reproducibility archive contains the LaTeX source, deterministic NumPy/SciPy implementation, a general-map diamond-norm SDP, exact SymPy certificates, JSON outputs, the figure source, a claim ledger, and SHA-256 hashes. No external data are used.

AI-assistance disclosure

The author used OpenAI Codex for repository and literature triage, proof exploration, symbolic and numerical code, and manuscript drafting. The claims are supplied with explicit proofs and reproducible certificates; responsibility for the submitted content remains with the author.

A Local word expansion and diamond remainder

For completeness, let

$$T_{j,\tau} = \mathcal{E}\,\mathrm{Ad}_{e^{-i\tau H_j}}\,\mathcal{E}, \qquad h_j = \mathcal{E}(H_j).$$

On $\mathcal{A}$,

$$T_{j,\tau} = I - i\tau\,\mathrm{ad}_{h_j} - \frac{\tau^2}{2}\mathcal{E}\,\mathrm{ad}^2_{H_j}\,\mathcal{E} + O_\diamond(\tau^3).$$

Multiplying a word and subtracting two permutations cancels all single-label terms. Each inverted pair contributes

$$[\mathrm{ad}_{h_j}, \mathrm{ad}_{h_k}] = \mathrm{ad}_{[h_j,h_k]} = -i\,\mathrm{ad}_{C_{jk}},$$

which proves (18). If $S = \sum_j \|H_j\|$, differentiating the product three times and using $\|\mathrm{ad}_H\|_\diamond \le 2\,\|H\|$ gives the explicit comparison remainder

$$\|R_{\sigma,\pi}(\tau)\|_\diamond \le \frac{8}{3}S^3|\tau|^3.$$

B Permutation-sign table

For $a < b < c$, enumerate the six relative orders. The three sign products in (22) are respectively

order	abc	acb	bac	bca	cab	cba	mean
$\varepsilon_{ab}\varepsilon_{ac}$	1	1	−1	1	−1	1	1/3
$\varepsilon_{ab}\varepsilon_{bc}$	1	−1	−1	−1	−1	1	−1/3
$\varepsilon_{ac}\varepsilon_{bc}$	1	−1	1	−1	1	1	1/3

For two disjoint pairs, swapping the labels of one pair is a sign-reversing involution that leaves the other sign fixed, hence their correlation is zero.

C Replay conventions

Superoperators use column-major vectorization. The numerical verifier uses seed 20260810. Absolute tolerances are 2×10^{-10} for generic covariance identities and 2×10^{-11} for sharp matrix equalities. Diamond norms are evaluated from the Choi matrix by a general-map semidefinite program, not by a state-only proxy. Random cases are regression evidence only; the analytic inequalities do not depend on sampling.

References

[1] L. Eriksson, "Operational Curvature of the Heisenberg Cut: Exact Diamond Readout, a Discrete Stokes Law, and Sharp Action Bounds for Dissipative Zeno Holonomy," submitted manuscript (2026).

[2] B. Misra and E. C. G. Sudarshan, "The Zeno's paradox in quantum theory," *J. Math. Phys.* **18**, 756–763 (1977). doi:10.1063/1.523304.

[3] P. Facchi and S. Pascazio, "Quantum Zeno dynamics: mathematical and physical aspects," *J. Phys. A* **41**, 493001 (2008). doi:10.1088/1751-8113/41/49/493001.

[4] D. Burgarth, P. Facchi, V. Giovannetti, H. Nakazato, S. Pascazio, and K. Yuasa, "Non-Abelian phases from quantum Zeno dynamics," *Phys. Rev. A* **88**, 042107 (2013). doi:10.1103/PhysRevA.88.042107.

[5] I. A. Luchnikov and S. N. Filippov, "Quantum evolution in the stroboscopic limit of repeated measurements," *Phys. Rev. A* **95**, 022113 (2017). doi:10.1103/PhysRevA.95.022113.

[6] E. Indrei and L. Nurbekyan, "On the stability of the polygonal isoperimetric inequality," *Adv. Math.* **276**, 62–86 (2015). doi:10.1016/j.aim.2015.02.013.

[7] P. Pai and F. Zhang, "Isoperimetric inequalities in quantum geometry," *Phys. Rev. Lett.* **136**, 116601 (2026). doi:10.1103/h9vk-lrvk.

[8] O. Sönnerborn, "Estimate of the time required to perform a nonadiabatic holonomic quantum computation," *Phys. Rev. A* **109**, 062433 (2024). doi:10.1103/PhysRevA.109.062433.

[9] O. Sönnerborn, "The isoholonomic inequality and tight implementations of holonomic quantum gates," *Phys. Rev. A* **111**, 052430 (2025). doi:10.1103/PhysRevA.111.052430.

[10] S. Tanimura, M. Nakahara, and D. Hayashi, "Isoholonomic problem and holonomic quantum computation," *J. Math. Phys.* **46**, 022101 (2005). doi:10.1063/1.1835545.

[11] J. G. Stampfli, "The norm of a derivation," *Pacific J. Math.* **33**, 737–747 (1970). doi:10.2140/pjm.1970.33.737.

[12] J. Watrous, "Semidefinite programs for completely bounded norms," *Theory Comput.* **5**, 217–238 (2009). doi:10.4086/toc.2009.v005a011.

[13] Y.-A. Chen, A. M. Childs, M. Hafezi, Z. Jiang, H. Kim, and Y. Xu, "Efficient product formulas for commutators and applications to quantum simulation," *Phys. Rev. Research* **4**, 013191 (2022). doi:10.1103/PhysRevResearch.4.013191.

[14] K. R. Dizaji, L. Kim, M. Marvian, and C. Arenz, "Higher-order Zeno sequences," *Phys. Rev. Research* **8**, 023051 (2026). doi:10.1103/glcd-gm3v.